# Regulation of Abnormal Expression of hsa_circRNA_0127523 on Proliferation, Migration and Invasion and miR-515-5p Expression in Oral Squamous Cell Carcinoma.

**Jianing Wei**
Laboratory Animal Center, Shanxi Key Laboratory of Experimental Animal Science and Human Disease Animal Model, Shanxi Medical University

**Zekun Wang**
State Key Laboratory of Oral Diseases, National Clinical Research Center for Oral Diseases, Department of Conservative Dentistry and Endodontics, West China Hospital of Stomatology, Sichuan University

**Jiping Gao**
Laboratory Animal Center, Shanxi Key Laboratory of Experimental Animal Science and Human Disease Animal Model, Shanxi Medical University

**Yuxiang Liang**
Laboratory Animal Center, Shanxi Key Laboratory of Experimental Animal Science and Human Disease Animal Model, Shanxi Medical University

**Guoqiang Xu**
Laboratory Animal Center, Shanxi Key Laboratory of Experimental Animal Science and Human Disease Animal Model, Shanxi Medical University

**Xiaotang Wang**
Laboratory Animal Center, Shanxi Key Laboratory of Experimental Animal Science and Human Disease Animal Model, Shanxi Medical University

**Lanfei Xiao**
Laboratory Animal Center, Shanxi Key Laboratory of Experimental Animal Science and Human Disease Animal Model, Shanxi Medical University

**Xiaoru Yan**
Laboratory Animal Center, Shanxi Key Laboratory of Experimental Animal Science and Human Disease Animal Model, Shanxi Medical University

**Guohua Song** ( ykdsgh@sxmu.edu.cn )
Laboratory Animal Center, Shanxi Key Laboratory of Experimental Animal Science and Human Disease Animal Model, Shanxi Medical University

---

**Research Article**

**Keywords:** oral squamous cell carcinoma, hsa_circ_0127523, cell proliferation, cell migration, cell invasion

**Posted Date:** January 11th, 2021

**DOI:** https://doi.org/10.21203/rs.3.rs-137128/v1

# Abstract

Circular RNA (circRNA) play an important role in many biological processes of occurrence and development of cancers. In this research, we established an animal model by DMBA-induced buccal sac tissue and discovered the differential expression of circRNAs by the second-generation sequencing. Models were identified by HE staining and ultrastructural observation. We found total of 3485 circRNAs were differentially expressed which the top 8 different expression circRNAs in sequencing results were confirmed by qRT-PCR. GO and KEGG analyses showed that differently expressed circRNAs function and pathway. Moreover, the axis relationship of circRNA-miRNA was predicted by miRanda. Silencing hsa_circ_0127523 significantly suppressed the proliferation, migration and invasion abilities of oral squamous cell carcinoma (OSCC) cells by RNAi, CCK-8, transwell migration and invasion assays. Furthermore, bioinformatics databases suggested that hsa_circ_0127523 might function by sponging miR-515-5p to regulate the expression of TRIP13. It was subsequently identified that hsa_circ_0127523 may inhibit miR-515-5p expression and increase TRIP13 expression in the OSCC cells. In summary, the results of the present study revealed that OSCC tissues have abundant circRNAs and we firstly explore the role of the hsa_circ_0127523 in the behavior regulation of OSCC cells. Its demonstrating that hsa_circ_0127523 may be a potential biomarker and therapeutic target of OSCC.


# Introduction

Oral cancer is the third leading cause of cancer-associated mortality worldwide [1], ranks sixth among the major causes of mortality [2]. Numerous factors account for the increasing incidence of oral squamous cell carcinoma (OSCC), including long-term addiction to tobacco and alcohol, long-term foreign body stimulation, poor oral hygiene habits and innutrition [3]. Each year approximately 600,000 new cases are diagnosed with only a 63% five-year survival rate [4–6]. In recent years, increasing attention has been paid to the diagnosis, treatment and prognosis of OSCC, however, the late detection and poor prognosis of OSCC is still a challenge. What's more, it's difficult to obtain clinical samples of different stages before cancer. Based on the above reasons, we made a dynamic carcinogenesis animal model using the Chinese hamsters. The Chinese hamster was selected as OSCC animal model has its own unique advantages: included a flexible cheek pouch on each side of the mouth that convenience for the operation of oral disease model drugs [7]. Therefore, the Chinese hamster buccal sac tissue tumor model is an ideal animal model for studying mechanical experiments, it's of significant significance to developing animal models with corresponding diseases using its unique structural advantages.

Non-coding RNA is a type of RNA transcript that cannot encode proteins after transcription, included microRNA (miRNA), long non-coding RNA (lncRNA) and circular RNA (circRNA) [8, 9]. They constitutes a competitive endogenous RNA (ceRNA) regulatory network. CircRNA is a novel special non-coding RNA, compared to traditional RNA, it's a covalently closed-loop RNA with no 3' polyadenylation tail and 5' cap, which is resistant to ribonuclease degradation and stably present in the cytoplasm and nucleus [10–13]. Besides, circRNA exhibit tissue-specific and highly conservative which is another new hot research in the non-coding RNA family following the reporting of miRNA and lncRNA. There are four mechanisms about

circRNA: the first is by acting as miRNA “molecular sponge” to regulate gene expression, the second is by regulating gene transcription, the third is interaction with protein and the fourth is participating in protein translation [10, 14, 15]. At present, there are researches on relevant mechanisms that Zhang et al has found circular AKT3 RNA encoded a novel tumor suppressor protein by competing with active phosphoinositide-dependent kinase-1 inhibits glioblastoma tumorigenity [16]. In addition, circ_SMARCA5 regulates glioblastoma multiforme through sponge SRSF1 protein [17]. What’s more, Xu et al has confirmed that the circTADA2As/miR-203a-3p/SOCS3 pathway modulates the progression and metastasis of breast cancer, and this pathway might be a promising target for the development of therapeutics for breast cancer [18].

Based on the above considerations, circRNA plays crucial roles in cancer by functioning as miRNA sponges and regulating mRNA translation. Therefore, we established dynamic oral squamous cell carcinogenesis animal model using the Chinese hamsters, and acquired circRNA differential expression profiling of OSCC by the next generation high-throughput sequencing, verified several significant differentially expression circRNA molecules which consistent with sequencing results. Additionally, we screened circRNA hsa_circ_0127523 (circMAN2A1) was markedly overexpressed by combine high-throughput sequencing with PCR verification. According to reports from related studies, Wang et al has found circDOCK1 affects the apoptosis of oral squamous cell carcinoma through the circDOCK1/miR-196a-5p/BIRC3 axis. The knockdown of the expression of circDOCK1 with small interfering RNA led to the increase of apoptosis. In addition, the protein expression level of BIRC3 was decreased when interfering with circDOCK1 expression in oral cancer cells of CAL27, SCC9 and SCC25 [19]. Hence, we explored the role of hsa_circ_0127523 in vitro OSCC cells. We designed and synthesized two siRNAs for the sequence near the cleavage site of hsa_circ_0127523, which were transiently transfected them into the OSCC cell lines to detect the expression levels of downstream target genes and proteins.

## Results

# HE staining of buccal sac tissues observe pathological structure.

Under the light microscope of normal buccal sac tissue, the spine cell layer of normal buccal pouch tissue was thin, the basal layer cells were clearly arranged neatly and the nail processes were not obvious. The histological observations of the blank control group and the negative control group were consistent and no abnormal changes occurred (Fig. 1a,b). The pathological structure of simple hyperplasia tissues group and abnormal hyperplasia tissues group is mild hyperemia of the buccal mucosa, pathological observation of atrophic cells thickening, basal layer cell proliferation and obvious changes, nail process is more obvious than the normal group (Fig. 1c,d). At cancer group, local leukoplakia lesions and erosion, pathological observation of spinous layer cells in a single or clustered keratosis, basal layer cell thickened, most of the basal cells abnormally proliferated, a large parts of cell polarity disappeared and arranged scatteredly (Fig. 1e).

# Transmission ultrastructure observation.

In ultrastructural observation, the shape of cell is closely arranged, the cell nucleus shape is regular, and the morphology of each organelle is normal and the desmosome is abundant which in normal group (Fig. 2a). Compared with the normal group, the morphology of the nucleus in some lesions changed, nucleoli edge gathered and desmosomes were relatively few in simple hyperplasia group (Fig. 2b); nuclei enlarged and condensed irregularly, desmosomes decreased mitochondrial edema in abnormal hyperplasia group (Fig. 2c); epithelial cells undergo canceration, cell shape changes, nuclear-cytoplasmic ratio decreases, and cancer cells invade connective tissue in squamous cell carcinoma group (Fig. 2d).

Based on the World Health Organization Cancer Diagnostic Criteria [20], oral precancerous lesion and oral squamous cell carcinoma are known to be induced in animal models after 9 and 15 weeks of drug treatment. Therefore, HE staining and ultrastructural observation of animal tissue samples confirmed the successful establishment of Chinese hamster animal model of OSCC. Thus, 12 samples were screened to high throughput sequencing, of which 3 samples were normal group, and the other 9 samples were simple hyperplasia group (n=3), abnormal hyperplasia group (n=3) and squamous cell carcinoma group (n=3).

# Validation of differential expression circRNAs.

To validate the differential expression circRNAs from the high-throughput sequencing results, which by quantitative real-time PCR (qRT-PCR) in tissue samples including the tissues that from high-throughput sequencing analysis. These include four up-regulated (cgr_circ_Gnaq, cgr_circ_Znf827, cgr_circ_Man2a1 and cgr_circ_Pdcd4) and four down-regulated (cgr_circ_Zeb1, cgr_circ_Me1, cgr_circ_Ankrd12 and cgr_circ_Akap7) circRNAs. The results showed that eight circRNA molecules were significantly dysregulation expression in simple hyperplasia tissues, abnormal hyperplasia tissues and carcinoma tissues (Fig. 3), which are the same as the results of sequencing (in Table 1).

Table 1
8 differently expresses circRNA molecules in the cheek pouch tissue of Chinese hamster.

| CircRNA-ID | $Log_2$Fold change | *P*-value | CircRNA type | Chrom | GeneSymbol | Threshold |
|---|---|---|---|---|---|---|
| 100689066 | 6.958839487 | 1.56E-05 | Exonic | Chr3 | Gnaq | UP |
| 100772729 | 5.294478448 | 0.032059 | Exonic | Chr3 | Znf827 | UP |
| 100757006 | 5.417308796 | 0.014185 | Exonic | Chr2 | Man2a1 | UP |
| 100766922 | 5.076242839 | 0.000302 | Exonic | Chr3 | Pdcd4 | UP |
| 100762046 | -1. 143693943 | 0.040624 | Exonic | Chr3 | Zeb1 | DOWN |
| 100767908 | -4.90997178 | 0.009489 | Exonic | Chr4 | Me1 | DOWN |
| 100755296 | -2.245709683 | 0.001166 | Exonic | Chr2 | Ankrd12 | DOWN |
| 100757731 | -4.115985224 | 0.036666 | Exonic | Chr2 | Akap7 | DOWN |
| Chrom: chromosome. | | | | | | |

# Elevated transfection efficiency of si-hsa_circ_0127523-1 and si-hsa_circ_0127523-2 by qRT-PCR in OSCC cells.

Hsa_circ_0127523 is encoded by the *MAN2A1* gene and located on chromosome 5 at chr5:109103235-109159538 and has a spliced sequence length of 1731 bp from UCSC and circBank database. The transfected cells were incubated for 48 hours, and the expression level of hsa_circ_0127523 was the gold standard for detecting the transfection efficiency. Our results showed that the expression level of hsa_circ_0127523 in the experimental group (Transient transfection si-hsa_circ_0127523-1 and si-hsa_circ_0127523-2 in OSCC cells) was significantly lower than that in the negative control group (Transient transfection si-NC in OSCC cells) ($P$<0.05), indicating that the interference efficiency was achieved (Fig. 4).

# Si-hsa_circ_0127523 inhibits proliferation ability of OSCC cells in vitro.

The effect of silencing hsa_circ_0127523 (si-hsa_circ_0127523-1 and si-hsa_circ_0127523-2) on the proliferation of CAL27 and Tca8113 cells was detected by CCK-8 assay, and the growth curve was drawn (Fig. 5). Our results showed that, the cell proliferation ability of CAL27 (Fig. 5a) and Tca8113 (Fig. 5b) cells after 3 and 2 days of silence respectively in hsa_circ_0127523 was significantly inhibited, compared with the control cells ($P$<0.05).

# Si-hsa_circ_0127523 inhibits migration and invasion of OSCC cells in vitro.

To examine the potential role of hsa_circ_0127523 in OSCC cell migration and invasion, we performed transwell assays in CAL27 and Tca8113 cells transfected with si-NC, si-hsa_circ_0127523-1 and si-hsa_circ_0127523-2. Compared with the negative control group, the results showed that si-hsa_circ_0127523-1 and si-hsa_circ_0127523-2 significantly inhibited migration (Fig. 6a) and matrigel invasion (Fig. 6b) of CAL27 and Tca8113 cells after 24 hours of culture ($P$<0.05), indicating hsa_circ_0127523 promoted the migration and invasion of CAL27 and Tca8113 cells.

# Hsa_circ_0127523 may interact with miRNA and mRNA.

In order to explore the mechanism and function of hsa_circ_0127523, investigated the potential interaction between circRNAs and miRNAs. By the online tools of CircInteractome, miRanda and Targetscan, we found that hsa_circ_0127523 may interact with hsa-miR-1200, hsa-miR-338-3p and miR-515-5p (Fig. 7a). Among them, the latest literature reports that miR-515-5p directly targeted TRIP13 3'-UTR and negatively correlated with TRIP13 mRNA expression in prostate cancer [21]. So, we examined the expression level of miR-515-5p and TRIP13 by qRT-PCR, found miR-515-5p was up-regulated and TRIP13 was down-regulated when silencing hsa_circ_0127523 (Fig. 7b,c). In addition, we found and tested the gene expression levels of Notch1 and p21 which by combine online software with literature. Also, the results showed that Notch1 and p21 were down-regulated when silenced hsa_circ_0127523 (Fig. 7d,e).

## Discussion

OSCC is one of the most common malignant tumors in the head and neck cancer. Its incidence is increasing year by year in the world, and the population of OSCC tends to be younger, which poses a serious threat to human health and life. Therefore, early detection and treatment of OSCC should not be delayed. So we build a dynamic animal model of OSCC in different stages, which can make up for the difficulty of obtaining samples in different clinical stages. In order to better prognosis treatment, it is important to elucidate the pathogenesis of OSCC. Non-coding RNA as a research hotspot in oncology, plays an important role in OSCC.

At present, the non-coding RNAs studied mainly include miRNA, lncRNA and circRNA [22]. Among them, miRNA and lncRNA are more mature, and circRNA is a hotspot in recent years. Compared with linear miRNA and mRNA, circRNA as a disease diagnostic marker has the unique advantages of high content and stable structure. Many studies on miRNAs and lncRNAs have been carried out and have demonstrated that these RNAs are related to oral squamous cell carcinoma proliferation, migration and invasion. Studies have shown that the miR-504 inhibiting cell proliferation, migration and invasion by regulating the expression of CDK6 in the process of OSCC [23]. Chen et al found that miRNA-10a promotes cancer cell proliferation in oral squamous cell carcinoma by regulating GLUT1 and promoting

glucose metabolism [24]. The literature reports that the lncRNA LUCAT1 might promote OSCC migration and invasion by regulating PCNA [25]. Moreover, some factors also regulate the function of ncRNA, for instance, Chen et al has pointed out NKILA has been shown to bind to the nuclear factor-kB (NF-kB)/IkB complex, which masks the phosphorylation sites of IkB, thus preventing its degradation [26]. It is well known that circRNA is stably present in vivo and vitro due to its covalently closed-loop structure. Consequently, using circRNA as a therapy target would better than miRNA and lncRNA.

Based on the above considerations, we established and validated oral squamous cell carcinoma animal model using Chinese hamster. Then we used RNA-seq technology to analyze the expression profiles of circRNA in tissues of OSCC at three different pathological stages and normal control tissues, and screen significantly different circRNAs in OSCC tissues. Our results pointed out that the expression of circRNA is abundant in twelve samples, including 3485 existing circRNA molecules and 229 novel circRNA molecules, 38 circRNAs were up-regulated while 51 were down-regulated in model group compared with control group. We selected four up-regulated and four down-regulated circRNAs for qRT-PCR validated that accordance with the high-throughput sequencing results. To the best of our knowledge, most of circRNAs were differentially expressed, indicating that these differentially expresses circRNAs might be implicated in the incidence and progression of OSCC. GO function and KEGG pathway analysis of the host genes of the significantly different circRNAs were used to predict related functions through bioinformatics. Based on the correlation between circRNA and its host gene and its known function, GO annotation analysis results show that GO term is mainly enriched in epithelial cell proliferation, actin-based cell projection and protein domain specific binding; KEGG further analysis shows that KEGG term is mainly enriched in Wnt, PI3K-Akt, MAPK, TGF-β, p53 and mTOR signaling pathways, revealing that the host genes of circRNAs may participate in the regulation of OSCC development through related molecular functions or signaling pathways. Besides important function and pathway, more and more studies have revealed that the mechanism of circRNAs sponge miRNAs [27, 28]. Finally, 35 abnormally expression circRNAs were selected to predict the circRNA-miRNA regulatory network from the perspective of ceRNA, which the potential biological functions were analyzed from the perspective of possible molecular mechanisms and revealed the important regulatory functions of circRNA in OSCC pathology. The above bioinformatics prediction analysis shows that these significantly different circRNAs have important regulatory roles in the pathology of OSCC, and are involved in promoting or inhibiting the occurrence and development of OSCC.

Due to the conservation and tissue specificity of circRNA, we screened up-regulated expressed cgr_circ_MAN2A1 in tissues by high-throughput sequencing. Therefore, we combined with bioinformatics databases (circBase, circBank and UCSC databases) and bioinformatics analysis to screen the gene of *MAN2A1* related circRNA, it was found that hsa_circ_0127523 is obtained by cleaving the pre-mRNA of *MAN2A1* and the full-length sequence of hsa_circ_0127523 was gotten. By detecting the expression level of the gene hsa_circ_0127523, it was found that the expression level of hsa_circ_0127523 in oral squamous cell carcinoma cell lines was significantly higher than that of normal cells. It is necessary to further study whether hsa_circ_0127523 plays an important regulatory role in OSCC. According to Ouyang et al research reports that circRNA_0109291 is highly expressed in oral squamous cell carcinoma and the

authors tested its functions and mechanisms by design to interfere with the circRNA_0109291 in OSCC [29]. Then, the behavioral function of hsa_circ_0127523 in CAL27 and Tca8113 cell lines shows that silencing hsa_circ_0127523 inhibited the proliferation, migration and invasion of OSCC cells in vitro.

It is well known that circRNAs play crucial roles in cancer by functioning as miRNA sponges, and affect the stability of target mRNA and regulate mRNA expression level [30, 31]. The latest literatures report the mechanism of circRNA to miRNA is a competitive endogenous mechanism, also called sponge mechanism [32], and the expression of circRNA and mRNA is positively correlated, the expression of circRNA and mRNA is negatively correlated with the expression of miRNA, which formed “circRNAs-miRNAs-mRNAs” target regulation network [33–35]. Studies have shown that hsa_circRNA_100533 act as a competitive endogenous RNA (ceRNA) and regulates the expression of GNAS by sponging has-miR-933, thereby modulating the proliferation, migration and apoptosis of OSCC [36]. By using a circRNA microarray, Gao et al demonstrated that circ-PKD2 as a ceRNA regulates APC2 expression by sponge miR-204-3p and participates in OSCC cell proliferation, migration and invasion, induced apoptosis and cell cycle arrest [37].

In our next study, the interaction network of hsa_circ_0127523 showed that it was most likely to regulate the expression of miR-515-5p according to the bioinformatics analysis. Further interaction analysis showed that the target gene of miR-515-5p most likely to affect the TRIP13 gene regulation. Therefore, we detected the expression of miR-515-5p and TRIP13 at the gene level after hsa_circ_0127523 was silenced, and found that the expression level of miR-515-5p decreased and TRIP13 increased after silencing hsa_circ_0127523. Moreover, Zhang et al found that TRIP13 as a direct target of miR-515-5p by binding to it’s 3’-UTR, which abolish the role of miR-515-5p in suppressing cell proliferation, migration and invasion that the miR-515-5p-TRIP13 axis may be a brightening prognostic marker and therapeutic target for prostate cancer [21]. TRIP13 (Thyriod hormone receptor interacting protein 13) is a nuclear factor, which is a protein-coding gene from the perspective of gene type. It is mainly involved in meiosis, cell proliferation and metastasis and is expressed in normal and cancerous tissues. Recent studies have found that it’s related to tumorigenesis, development and prognosis [38, 39]. Kurita et al [40] found through research that TRIP13 is highly expressed in cancer tissues of colorectal cancer patients and the deletion of the TRIP13 gene can inhibit cancer cell proliferation, migration and invasion, which may become a potential target for colorectal cancer treatment. In addition, TRIP13 gene is abnormally highly expressed in head and neck malignancies, multiple myeloma, chronic lymphocytic leukemia and lung adenocarcinoma [41–43], which may be related to the occurrence and development of malignant tumors. There are no reports about the study of TRIP13 in OSCC. Therefore, this study hopes to provide valuable reference for clinical treatment from the perspective of TRIP13. Our study forecasted the sponge mechanisms of hsa_circ_0127523/miR-515-5p/TRIP13 axis in OSCC, which verified the differential expression level that are coincidence with competitive endogenous mechanism.

In addition, the expression level of Notch1 and p21 were abnormal when inhibited the expression level of hsa_circ_0127523 in OSCC cells, current studies have suggested that hsa_circ_0127523 may regulate the occurrence and development of OSCC through Notch pathway. Role of TRIP13 has been reported in the

literature, and related research validation has also suggested that TRIP13 gene affects the expression levels of Notch1 and p21 in the Notch pathway in ovarian cancer [21, 44]. Analysis by Yoshida et al reported that Notch1 plays a vital role in the development and progress of OSCC. Based on deep sequencing of the cancer genome, research has also suggested the anti-cancer effect of Notch1. Notch plays an indispensable role in OSCC because Notch is considered to play an oncogene role in a subset of OSCC and also has a suppressive effect [45]. Lv et al has found that miR-495 restricts the proliferation and invasion of OSCC cells by directly targeting Notch1. Notch1 knockdown shows an inhibitory effect similar to that induced by miR-495 overexpression in OSCC cells [46]. Cyclin-dependent kinase (CDK) and cyclin-dependent kinase inhibitor (CDKI) can directly control the cell cycle. p21 is a negative regulator of cyclin-dependent kinases and is a negative checkpoint regulator of the cell cycle in this function [47]. Previous studies have shown that p21 is over expressed in lung cancer and gastrointestinal cancer cells [48, 49].The results of Zhang's study show that the 5-year survival rate of OSCC patients with high p21 expression is significantly reduced. Kaplan-Meier analysis and Cox proportional hazard model showed that lymph node metastasis and p21 expression were independent prognostic factors of OSCC [50], which are consistent with our findings that silenced the hsa_circ_0127523, the TRIP13 expression level was decreases and the Notch1 decreases in the Notch pathway.

Increasing studies suggest that circRNA has a vital part in a variety of tumors as a tumor regulator. As reported by Su that hsa_circ_0055538 could regulate the malignant biological behavior of OSCC through the p53/Bcl-2/caspase signaling pathway [51]. And it has been reported that circDOCK1 suppresses cell apoptosis via inhibition of miR-196a-5p by targeting BIRC3 in OSCC [19]. Chen et al found that circRNA_100290 was bound to miR-29 family members directly and co-expressed with CDK6 influenced proliferation in oral cancer cell [52]. In non-small cell lung cancer, Huang et al demonstrated that hsa_circ_0001946 may serve as a novel biomarker for the diagnosis and prediction of platinum-based chemosensitivity in patients with NSCLC [53]. Sang et al has identificated that hsa_circ_0025202 served an anti-oncogenic role in HR-positive breast cancer, could suppress tumor growth and enhance tamoxifen efficacy, and it could be exploited as a novel marker for breast cancer [54]. Based on these, we propose a view that circRNA may participate in development and prognosis of OSCC and our study showed that hsa_circ_0127523/miR-515-5p/TRIP13 by modulated Notch pathway may play an important role in OSCC cancer development. However, hsa_circ_0127523 has not been reported in the any disease, so it is concluded that hsa_circ_0127523 may be a potential biomarker of OSCC. In the next study, we will further elucidate the regulatory mechanism of hsa_circ_0127523/miR-515-5p/TRIP13 in OSCC.

In conclusion, our study provided evidence that oral circRNAs are differentially expressed in response to OSCC. In the expression signatures, we uncovered the circRNAs expression profile in three dynamic stages by comparing it with normal tissue. Additionally, eight dysregulated circRNAs expression level in tissue were verified by qRT-PCR, which is consistent with the sequencing result. Additionally, we confirmed hsa_circ_0127523 was interfered significantly affected the proliferation, migration and invasion abilities of OSCC cells. More important, we predicted and confirmed hsa_circ_0127523 inhibit miR-515-5p expression and increase TRIP13 expression in the OSCC cells which provide potential axis for the next

step diagnosis of OSCC and novel genetic insights, and the specific mechanism still needs further research. Hsa_circ_0127523 may be a potential marker and therapeutic target for the diagnosis of OSCC.

## Materials And Methods

# Construction of animal model.

Chinese hamsters (n=90) were individually housed in cages with standard laboratory conditions at 25°C, 45% humidity, controlled environment with a 12-hour light/dark cycles. They were randomly divided into three groups: control group (n=30, not any treated), negative control group (n=12, coated with acetone) and model group (n=48, coated with acetone-dissolved 9, 10-Dimethy1-1, 2-Benzanthracence (DMBA)) [55]. After applying, the Chinese hamsters were fasted for 2 hours after the application, and the rest was free to eat and drink. Anatomical samples were performed regularly at weeks 6, 9, 12, 15, 18 and 21: the Chinese hamsters were anesthetized with 0.3% pentobarbital sodium solution by intraperitoneal injection, the left and right cheek pouches of the Chinese hamster were taken, which 1/2 buccal sac tissues were marked and placed in liquid nitrogen for freezed immediately, and then stored at -80°C in the refrigerator; 1/4 buccal sac tissues were fixed in 4% paraformaldehyde for 24 hours, then subjected to alcohol gradient dehydration, paraffin embedding; 1/4 buccal sac tissues were quickly placed in a glutaraldehyde fixative solution and fixed at 4°C. Animal experiments were performed at barrier animal laboratory facility of the Center for Experimental Animal of Shanxi Medical University [SCXK (Jin) 2017-0001] and carried out strictly in accordance with the operating rules formulated by the Institutional Animal Care and Use Committee of Shanxi Medical University (IACUC 2017-016). According to the 3R principle (Reduction, Replacement and Refinement) used by the experimental animals, humane care is given.

# HE staining to detect pathologic structure.

The paraffin-embedded tissues were subjected to alcohol gradient and xylene dewaxing treatment, 4 $\mu$m longitudinal sections were stained with hematoxylin solution for 3 minutes, then rinsed in distilled water twice. Immerse the slice in the 1% acid ethanol for 1 minute and rinse with distilled water. Then the sections were stained with eosin solution for 2 minutes and followed by rinsing in distilled water and dehydration with graded alcohol and clearing in xylene. Finally, the pathological results were observed under a fluorescence microscope (IX70, Olympus).

# Ultrastructural observation by Scanning Transmission Electron Microscopy (STEM).

The buccal sac tissue fixed by glutaraldehyde was immersed in phosphate buffer solution, then immobilized in osmium tetroxide solution, dehydrated by ethanol gradient, and embedded in epoxy resin

No. 812. After polymerization, the buccal sac tissue was sliced by ultrathin slice machine, stained with uranyl acetate and lead citrate, and observed by transmission electron microscopy under a microscope.

# RNA extraction and quality test.

Total RNAs were extracted from frozen tissues and OSCC cells using miRNeasy Mini Kit (External content QIAzol Lysis Reagent), according to the manufacturer's instructions. Then the RNA qualities were evaluated by NanoDrop ND-1000 spectrophotometer (Thermo Fisher Scientific, USA). The RNA purity is qualified by the OD260/OD280 ratio, which ranges from 1.8 to 2.0, and RNA integrity was assessed by 1% agarose gel electrophoresis analysis. Total miRNA was extracted from the OSCC cells using miRNA extraction and purification kits, preserved at -80℃ before using.

# Library construction and sequencing.

After RNA extraction and quality test, a quantity of 1 μg total RNA of tissues was constructed library, using TruSeq Small RNA Library Prep Kit for Illumina following the manufacturer's protocol. Removed ribosomes RNAs, enriched circRNAs were short fragment by using fragmentation buffer. First strand cDNA was synthesized using reverse transcriptase with random hexamer primers. Second strand cDNA was synthesized by DNA polymerase I, dNTP, RNase H. Next, the cDNA fragments were purified with AMPure XP beads. The purified double-stranded cDNA was repaired end, poly(A) added and ligated to Illumina sequencing connector, then, AMPure XP beads were used to select the fragment size, the target fragment was recovered by agarose gel electrophoresis. The obtained fragment was subjected to PCR amplification and enrichment, the cDNA library was constructed. The constructed cDNA library was quantified using Qubit2.0. Which was tested by Agilent 2100 Bioanalyzer and ABI StepOne plus Real-time PCR System. After passing the quality inspection, the effective concentration of the library (more than 2nM) was quantified accurately by qPCR to ensure the quality of the library. Sequenced using Illumina Hiseq2500 SR50. Each sample was blasted to the genome by quality-controlled PE clean reads data and the Chinese hamster reference genome (GCF_000223135.1_GriGri_1.0_genomic.fa, NCBI). The comparison software uses the BWA-MEM algorithm required by CIRI, a circular RNA identification tool.

# CircRNA expression standardization and data analysis.

All raw reads were obtained from the sequencing machines. The absolute expression of circular RNA is generally measured by detecting the number of sequences aligned to the head-to-tail locus, but since the total amount of sequencing of each sample library is different, so standardization is required. The RPM (read per million) method commonly used in data analysis was used to normalize the expression level of circular RNA. According to the screening threshold of RPM>0.1, a total of 3485 circRNAs were obtained that satisfied the expression requirements. Differential expression analysis of model and control groups was performed using edgeR package. We identified circRNAs with $\log_2$ |(Fold change)|>2 and *P*-value

<0.05 as significant differentially expressed circRNAs, then circRNAs were annotated with *Cricetulus griseus* genome. Those cannot be annotated were defined as novel circRNAs.

# Functional enrichment and pathway analysis.

During functional enrichment analysis of differentially expressed circRNAs, the online analysis tool-Metascape was utilized to perform gene ontology (GO) enrichment analysis. Kyoto Encyclopedia of Genes and Genomes pathway (KEGG) analysis associated genes of differentially expressed circRNA.

# Integrated analysis of circRNAs-miRNAs in Chinese hamster tissue.

The target relationship of annotated circRNAs with miRNAs were theoretically predicted by conserved seed-matching sequence using miRanda (v3.3a) analysis, which the maximum binding energy required is less than -20, and there are at least two miRNA binding sites on a circular RNA sequence. The analysis showed all circRNAs contained their respective miRNA response elements (MREs) and the circRNA-miRNA network was visualized by Cytoscape 3.01.

# Cells culture.

The human cell lines CAL27 and Tca8113 were purchased from Procell and Boster Biological Technology (Wuhan, China). OSCC cell lines were cultured in DMEM medium supplemented with 10% fetal bovine serum and 1% penicillin/streptomycin. All cells were cultured at 37℃ with 5% $CO_2$.

# RNA interference and transient cell transfection.

The small interfering RNA (siRNA) and negative control siRNA (si-NC) were synthesized by GenePharma (Shanghai, China) to inhibit the expression of hsa_circ_0127523 in CAL27 and Tca8113 cells. Si-hsa_circ_0127523 siRNA (si-hsa_circ_0127523-1: sense: 5′-ACAUACAGGGAGUGAAACCTT-3′; antisense: 5′-GGUUUCACUCCCUGUAUGUTT-3′; si-hsa_circ_0127523-2: sense: 5′-UAUACCACAUACAGGGAGUTT-3′; antisense:5′- ACUCCCUGUAUGUGGUAUATT-3′) and negative control siRNA (si-NC:sense: 5′-UUCUCCGAACGUGUCACGUTT-3′; antisense: 5′-ACGUGACACGUUCGGAGAATT-3′) were transfected into CAL27 and Tca8113 cells using Lipofectamine RNAiMAX Reagent (Thermo Fisher Scientific, USA). After the operation, place the 6-well plate in the incubator as soon as possible. Transfection sequence after inoculation of cells for 24 hours.

# Quantitative Real-Time Polymerase Chain Reaction (qRT-PCR).

Total RNA was reverse transcribed to cDNA by random hexamer primers (Takara, Japan). SYBR green PCR Master Mix (Takara, Japan) was used to examine circRNA, miRNA and mRNA expression, circRNAs and mRNAs using glyceraldehyde-3-phosphate dehydrogenase (GAPDH) as an endogenous control, miRNAs using U6 as an endogenous control, every group at least three tissues and repeat at least three times, which monitored by the ABI StepOne Plus Real-time PCR System. The melting curve insure the specificity of primers. Relative circRNAs, miRNAs and mRNAs expression were calculated according to the $2^{-\Delta\Delta CT}$ method. The primers were designed and synthesized by using Oligo 6.0 software and Shanghai Sangon Biotech (Table 2, 3).

Table 2
Primers of circRNA sequences from cheek pouch tissues of Chinese hamster.

| Gene Symbol | CircRNA | Primer type | Primer sequence(5'-3') | TM | Amplicon length |
|---|---|---|---|---|---|
| Gnaq | Cgr-circ-Gnaq | F primer | TGCCCCTCAACTGAAGAATGGA | 58.6°C | 189 bp |
| | | R primer | TGCATGCATCAGATGTGTGCT | 57.4°C | 189 bp |
| Znf827 | Cgr-circ-Znf827 | F primer | GAAGCCATGCTGCACGGAAG | 60.2°C | 115 bp |
| | | R primer | TGGAGACTGGGGAGTCCTGG | 61.8°C | 115 bp |
| Man2a1 | Cgr-circ-Man2a1 | F primer | CTGATGAAGCCACCGCACAC | 59.5°C | 196 bp |
| | | R primer | CCTCCACAGACTCGCTCAGG | 61.5°C | 196 bp |
| Pdcd4 | Cgr-circ-Pdcd4 | F primer | AAGCGAAGGAGATGGAGGCC | 60.6°C | 200 bp |
| | | R primer | ACCAGTGGCGTTTACATTCAGA | 56.4°C | 200 bp |
| Zeb1 | Cgr-circ-Zeb1 | F primer | CGCAGATGCAGCTGACTGTG | 59.8°C | 154 bp |
| | | R primer | TCAGCCAATTGCCAGTTGAGA | 56.9°C | 154 bp |
| Me1 | Cgr-circ- Me1 | F primer | ATTGGGCTGCGACAGAGGAG | 59.5°C | 144 bp |
| | | R primer | AGCTAGGTGGCAGCAATCCA | 57.5°C | 144 bp |
| Ankrd12 | Cgr-circ-Ankrd12 | F primer | TGCTTGATCAAAGTGCCTCAAGG | 57.9°C | 180 bp |
| | | R primer | ACCTTTCTTCCGTATGGCCTCT | 58.1°C | 180 bp |
| Akap7 | Cgr-circ-Akap7 | F primer | CTGTACCAGATAGATCTCTGCTCCA | 57.3°C | 147 bp |
| | | R primer | TCTAATTCCCCTGACACCGTCTC | 58.4°C | 147 bp |
| F: forward R: reverse. | | | | | |

Table 3
Primers of circRNA and miRNA sequences of OSCC cell.

| Primer | Sequence (5'-3') |
|---|---|
| hsa_circ_0127523 | GAGACAGAATTGGGATCTGGGA (forward primer) |
| | AAGGCTTGGCATTACCATCAGG (reverse primer) |
| GAPDH | AGGTATCCTGACCCTGAAGT (forward primer) |
| | GCTCGTTGCCAATAGTGAT (reverse primer) |
| U6 | GCGCGTCGTGAAGCGTYC (forward primer) |
| | GTGCAGGGT-CCGAGGT (reverse primer) |
| hsa-miR-515-5p | UUCUCCAAAAGAAAGCACUUUCUG |
| TRIP13 | ACTGTTGCACTTCACATTTTCCA (forward primer) |
| | TCGAGGAGATGGGATTTGACT (reverse primer) |
| Notch1 | GCCGCCGCCGTGAACAATG (forward primer) |
| | GCCGCCGCCGTGAACAATG (reverse primer) |
| p21 | CTCTCAACGACAGCAGCCCG (forward primer) |
| | AGGTGATCCAGACTCTGACC (reverse primer) |

# Cell Counting Kit-8 (CCK-8) assay.

The proliferation of CAL27 and Tca8113 cells were detected by the CCK-8 assay. Infected cells were plated into 96-well plates at $3\times10^3$ cells/well. At 0, 24, 48 and 72 hours, according to the manufacturer's guidelines, 10 μl of CCK-8 liguid (Boster Biological Technology, Wuhan, China) was added adherence and incubation for 2 hours. The optical density (OD) was detected by a microplate reader at 450 nm.

# Transwell migration and matrigel invasion assays.

The migration and matrigel invasion assays were performed using 24-well transwell plates, using transwell chamber and pre-coated matrigel transwell chamber respectively. The infected cells were suspension in DMEM without FBS and added to the upper chambers ($2\times10^4$ cells in 200 μl medium), while the lower chambers were added DMEM including 10% FBS (700 μl) and incubated for 48 hours. Compared with the upper chambers of migration assay, the upper chamber of invasion assay was added with matrigel. After incubation 48 hours, the cells and matrigel in upper chambers were removed, the cells which migration or invasion were fixed 30 minutes in 4% paraformaldehyde and stained 1 hour with 0.1% crystal violet, taken photos and counted.

# Online prediction in human cells.

CircRNA-miRNA interaction was predicted with the software CircInteratome (https://circinteractome.nia.nih.gov), miRanda (http://www.microrna.org/microrna/microrna/home.do) and Targetscan (http://www.targetscan.org/vert_72).

# Statistical analysis.

All data were statistical analyses by SPSS 22.0 and GraphPad Prism 8.0 software. Demonstrate significant difference circRNAs from high-throughput sequencing were analyzed by *t*-test between model and control groups. The results of PCR, CCK-8, migration and invasion were presented as mean ± SEM. Statistically significant data ($P$<0.05) were determined by Student t-test. The pairwise comparison between the multiple groups of samples was performed by the LSD method in one-way analysis of variance (ANOVA).

## Declarations

# Availability of materials and data

All data generated or analyzed during this study are included in this published article.

# Acknowledgements

The author thanks Shanxi Laboratory Animal Center and Shanxi Key Laboratory of Experimental Animal Science and Human Disease Animal Model, Shanxi Medical University. This work was funded by the National Natural Science Foundation of China (grant number 31772551; 31970513).

# Authors' contributions

J.N.W, G.Q.X and G.H.S carried out the studies, participated in the established animal model and drafted the manuscript. Z.K.W, Y.X.L, X.T.W, L.F.X and X.R.Y carried out the collected samples and processed samples. J.N.W, Z.K.W and J.P.G participated in the design of the study and performed the statistical analysis. All authors read and approved the final manuscript.

# Ethics approval and consent to participate

The Ethics Committee of the Shanxi Medical University reviewed and approved all research procedures involving animal participants.

# Competing interests

All of the authors have announced that there was no conflict of interest in this work.

# Statement

This study was carried out in compliance With the ARRIVE guidelines. All animal experiments and methods were performed in accordance with relevant guidelines and regulations.

## References


1. Wang, Y. F. *et al*. Induction of autophagy-dependent cell death by the survivin suppressant YM155 in salivary adenoid cystic carcinoma. *Apoptosis*. **19,** 748-758 (2014).
2. Sasahira, T. *et al*. HuD promotes progression of oral squamous cell carcinoma. *Pathobiology : journal of immunopathology, molecular and cellular biology*. **81,** 206-214 (2014).
3. Thiagarajan, S. *et al*. Patterns of failure and outcomes in cT4 Oral squamous cell carcinoma (OSCC) undergoing upfront surgery in comparison to Neo-Adjuvant Chemotherapy (NACT) followed by surgery: A Matched Pair analysis. *Oral oncology*. **100,** 104455, https://doi.org/10.1016/j.oraloncology.2019.104455 (2020).
4. Kuo, Y. Y. *et al*. Caffeic Acid phenethyl ester is a potential therapeutic agent for oral cancer. *International journal of molecular sciences*. **16,** 10748-10766 (2015).
5. Zhang, L. *et al*. Dual induction of apoptotic and autophagic cell death by targeting survivin in head neck squamous cell carcinoma. *Cell death & disease*. **6,** e1771, https://doi.org/10.1038/cddis.2015.139 (2015).
6. Keshavarzi, M. & Darijani, M. Molecular Imaging and Oral Cancer Diagnosis and Therapy. *J Cell Biochem*. **118,** 3055-3060 (2017).
7. Xu, G. Q. *et al*. Identification and profiling of microRNAs expressed in oral buccal mucosa squamous cell carcinoma of Chinese hamster. *Scientific reports*. **9,** 15616, https://doi.org/10.1038/s41598-019-52197-3 (2019).
8. Taulli, R., Loretelli, C. & Pandolfi, P. P. From pseudo-ceRNAs to circ-ceRNAs: a tale of cross-talk and competition. *Nature structural & molecular biology*. **20,** 541-543 (2013).
9. Zhao, Z. J. & Shen, J. Circular RNA participates in the carcinogenesis and the malignant behavior of cancer. *RNA biology*. **14,** 514-521 (2017).
10. Li, X., Yang, L. & Chen, L. L. The Biogenesis, Functions, and Challenges of Circular RNAs. *Molecular cell*. **71,** 428-442 (2018).
11. Lasda, E. & Parker, R. Circular RNAs: diversity of form and function. *RNA (New York, NY)*. **20,** 1829-1842 (2014).

12. Wilusz, J. E. A 360° view of circular RNAs: From biogenesis to functions. *Wiley interdisciplinary reviews RNA*. **9,** e1478, https://doi.org/10.1002/wrna.1478 (2018).
13. Chen, L. L. & Yang, L. Regulation of circRNA biogenesis. *RNA biology*. **12,** 381-388 (2015).
14. Li, Y. *et al*. Computational identifying and characterizing circular RNAs and their associated genes in hepatocellular carcinoma. *PloS one*. **12,** e0174436, https://doi.org/10.1371/journal.pone.0174436 (2017).
15. Dong, Y. *et al*. Circular RNAs in cancer: an emerging key player. *Journal of hematology & oncology*. **10,** 2, https://doi.org/10.1186/s13045-016-0370-2 (2017).
16. Xia, X. *et al*. A novel tumor suppressor protein encoded by circular AKT3 RNA inhibits glioblastoma tumorigenicity by competing with active phosphoinositide-dependent Kinase-1. *Molecular cancer.* **18,** 131, https://doi.org/10.1186/s12943-019-1056-5 (2019).
17. Barbagallo, D. Caponnetto, A. Brex, D. Mirabella, F. & Barbagallo, C. CircSMARCA5 Regulates VEGFA mRNA Splicing and Angiogenesis in Glioblastoma Multiforme Through the Binding of SRSF1. *Cancers*. **11,** 194, https://doi.org/10.3390/cancers11020194 (2019).
18. Xu, J. Z. *et al*. circTADA2As suppress breast cancer progression and metastasis via targeting miR-203a-3p/SOCS3 axis. *Cell death & disease*. **10,** 175, https://doi.org/10.1038/s41419-019-1382-y (2019).
19. Wang, L. *et al*. CircDOCK1 suppresses cell apoptosis via inhibition of miR-196a-5p by targeting BIRC3 in OSCC. *Oncology reports*. **39,** 951-966 (2018).
20. Kramer, I. R., Lucas, R. B., Pindborg, J. J. & Sobin, L. H. Definition of leukoplakia and related lesions: an aid to studies on oral precancer. *Oral surgery, oral medicine, and oral pathology*. **46,** 518-539 (1978).
21. Zhang, X., Zhou, J., Xue, D., Li, Z., Liu, Y. & Dong, L. MiR-515-5p acts as a tumor suppressor via targeting TRIP13 in prostate cancer. *International journal of biological macromolecules*. **129,** 227-232 (2019).
22. Qu, S. *et al*. Circular RNA: A new star of noncoding RNAs. *Cancer letters*. **365,** 141-148 (2015).
23. Wang, X. *et al*. MicroRNA-504 functions as a tumor suppressor in oral squamous cell carcinoma through inhibiting cell proliferation, migration and invasion by targeting CDK6. *The international journal of biochemistry & cell biology*. **119,** 105663, https://doi.org/10.1016/j.biocel.2019.105663 (2020).
24. Chen, Y. H., Song, Y., Yu, Y. L., Cheng, W. & Tong, X. miRNA-10a promotes cancer cell proliferation in oral squamous cell carcinoma by upregulating GLUT1 and promoting glucose metabolism. *Oncology letters*. **17,** 5441-5446 (2019).
25. Kong, Y. *et al*. LncRNA LUCAT1 promotes rowth, migration, and invasion of oral squamous cell carcinoma by upregulating PCNA. *European review for medical and pharmacological sciences*. **23,** 4770-4776 (2019).
26. Chew, C. L., Conos, S. A., Unal, B. & Tergaonkar, V. Noncoding RNAs: Master Regulators of Inflammatory Signaling. *Trends in molecular medicine*. **24,** 66-84 (2018).

27. Kulcheski, F. R., Christoff, A. P. & Margis, R. Circular RNAs are miRNA sponges and can be used as a new class of biomarker. *Journal of biotechnology*. **238,** 42-51 (2016).
28. Ryu, J. *et al*. Characterization of Circular RNAs in Vascular Smooth Muscle Cells with Vascular Calcification. *Molecular therapy Nucleic acids*. **19,** 31-41 (2020).
29. Ouyang, S. B., Wang, J., Zhao, S. Y., Zhang, X. H. & Liao, L. CircRNA_0109291 regulates cell growth and migration in oral squamous cell carcinoma and its clinical significance. *Iranian journal of basic medical sciences*. **21,** 1186-1191 (2018).
30. Yuan, D. M., Ma, J., Fang, W. B. Identification of non-coding RNA regulatory networks in pediatric acute myeloid leukemia reveals circ-0004136 could promote cell proliferation by sponging miR-142. *European review for medical and pharmacological sciences*. **23,** 9251-9258 (2019).
31. Yang, J. *et al*. Curcumin enhances radiosensitization of nasopharyngeal carcinoma by regulating circRNA network. *Molecular carcinogenesis*. **59,** 202-214 (2020).
32. Mendell, J. T. & Olson, E. N. MicroRNAs in stress signaling and human disease. *Cell*. **148,** 1172-1187 (2012).
33. Rong, D. *et al*. An emerging function of circRNA-miRNAs-mRNA axis in human diseases. *Oncotarget*. **8,** 73271-73281 (2017).
34. Greene, J. *et al*. Circular RNAs: Biogenesis, Function and Role in Human Diseases. *Frontiers in molecular biosciences*. **4,** 38, https://doi.org/10.3389/fmolb.2017.00038 (2017).
35. Yang, G., Zhang, Y. & Yang, J. Identification of Potentially Functional CircRNA-miRNA-mRNA Regulatory Network in Gastric Carcinoma using Bioinformatics Analysis. *Medical science monitor : international medical journal of experimental and clinical research*. **25,** 8777-8796 (2019).
36. Zhu, X., Shao, P., Tang, Y., Shu, M. & Hu, W. W. Hsa_circRNA_100533 regulates GNAS by sponging hsa_miR_933 to prevent oral squamous cell carcinoma. *Journal of cellular biochemistry*. **120,** 19159-19171 (2019).
37. Gao, L. *et al*. Circ-PKD2 inhibits carcinogenesis via the miR-204-3p/APC2 axis in oral squamous cell carcinoma. *Molecular carcinogenesis.* **58,** 1783-1794 (2019).
38. Sudakin, V., Chan, G. K. & Yen, T. J. Checkpoint inhibition of the APC/C in HeLa cells is mediated by a complex of BUBR1, BUB3, CDC20, and MAD2. *The Journal of cell biology*. **154,** 925-936 (2001).
39. Tipton, A. R., Tipton, M., Yen, T. & Liu, S. T. Closed MAD2 (C-MAD2) is selectively incorporated into the mitotic checkpoint complex (MCC). *Cell cycle (Georgetown, Tex)*. **10,** 3740-3750 (2011).
40. Kurita, K. *et al*. TRIP13 is expressed in colorectal cancer and promotes cancer cell invasion. *Oncology letters*. **12,** 5240-5246 (2016).
41. Kass, E. M. & Jasin, M. Collaboration and competition between DNA double-strand break repair pathways. *FEBS letters*. **584,** 3703-3708 (2010).
42. Holloman, W. K. Unraveling the mechanism of BRCA2 in homologous recombination. *Nature structural & molecular biology*. **18,** 748-754 (2011).

43. Zhou, W. *et al*. NEK2 induces drug resistance mainly through activation of efflux drug pumps and is associated with poor prognosis in myeloma and other cancers. *Cancer cell*. **23,** 48-62 (2013).
44. Zhou, X. Y., Shu, X. M. TRIP13 promotes proliferation and invasion of epithelial ovarian cancer cells through Notch signaling pathway. *European review for medical and pharmacological sciences*. **23,** 522-529 (2019).
45. Yoshida, R., Ito, T., Hassan, W. A. & Nakayama, H. Notch1 in oral squamous cell carcinoma. *Histology and histopathology*. **32,** 315-323 (2017).
46. Lv, L., Wang, Q., Yang, Y. & Ji, H. MicroRNA-495 targets Notch1 to prohibit cell proliferation and invasion in oral squamous cell carcinoma. *Molecular medicine reports*. **19,** 693-702 (2019).
47. Fillies, T. *et al*. Cell cycle regulating proteins p21 and p27 in prognosis of oral squamous cell carcinomas. *Oncology reports*. **17,** 355-359 (2007).
48. Yin, D. *et al*. Long noncoding RNA AFAP1-AS1 predicts a poor prognosis and regulates non-small cell lung cancer cell proliferation by epigenetically repressing p21 expression. *Molecular cancer*. **17,** 92, https://doi.org/10.1186/s12943-018-0836-7 (2018).
49. Xu, J. *et al*. EZH2 promotes gastric cancer cells proliferation by repressing p21 expression. *Pathology, research and practice*. **215,** 152374, https://doi.org/10.1016/j.prp.2019.03.003 (2019).
50. Zhang, M. *et al*. Prognostic significance of p21, p27 and survivin protein expression in patients with oral squamous cell carcinoma. *Oncology letters*. **6,** 381-386 (2013).
51. Su, W., Sun, S., Wang, F., Shen, Y. & Yang, H. Circular RNA hsa_circ_0055538 regulates the malignant biological behavior of oral squamous cell carcinoma through the p53/Bcl-2/caspase signaling pathway. *Journal of translational medicine*. **17,** 76, https://doi.org/10.1186/s12967-019-1830-6 (2019).
52. Chen, L. *et al*. Retraction Note: circRNA_100290 plays a role in oral cancer by functioning as a sponge of the miR-29 family. *Oncogene*. **38,** 5750, https://doi.org/10.1038/s41388-019-0828-0 (2019).
53. Huang, M. S. *et al*. Hsa_circ_0001946 Inhibits Lung Cancer Progression and Mediates Cisplatin Sensitivity in Non-small Cell Lung Cancer via the Nucleotide Excision Repair Signaling Pathway. *Frontiers in oncology*. **9,** 508, https://doi.org/10.3389/fonc.2019.00508 (2019).
54. Sang, Y. *et al*. CircRNA_0025202 Regulates Tamoxifen Sensitivity and Tumor Progression via Regulating the miR-182-5p/FOXO3a Axis in Breast Cancer. *Molecular therapy : the journal of the American Society of Gene Therapy*. **27,** 1638-1652 (2019).
55. Mahakian, L. M. *et al*. Comparison of PET imaging with 64Cu-liposomes and 18F-FDG in the 7,12-dimethylbenz[a]anthracene (DMBA)-induced hamster buccal pouch model of oral dysplasia and squamous cell carcinoma. *Molecular imaging and biology*. **16,** 284-292 (2014).

# Figures

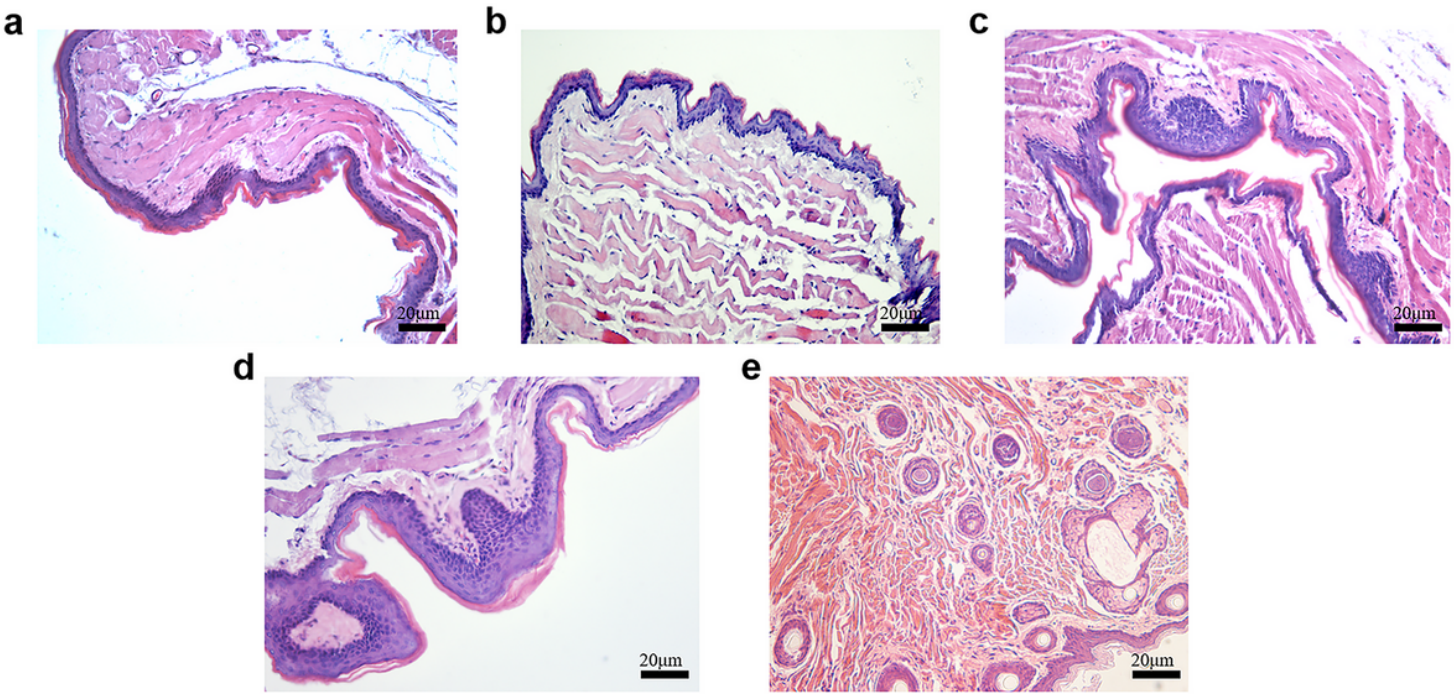


**Figure 1**

HE staining pathologic structure(×200). (a) Pathologic structure of blank control tissues. (b) Pathologic structure of negative control tissues. (c) Pathologic structure of simple hyperplasia tissues. (d) Pathologic structure of abnormal hyperplasia tissues. (e) Pathologic structure of carcinoma tissues.

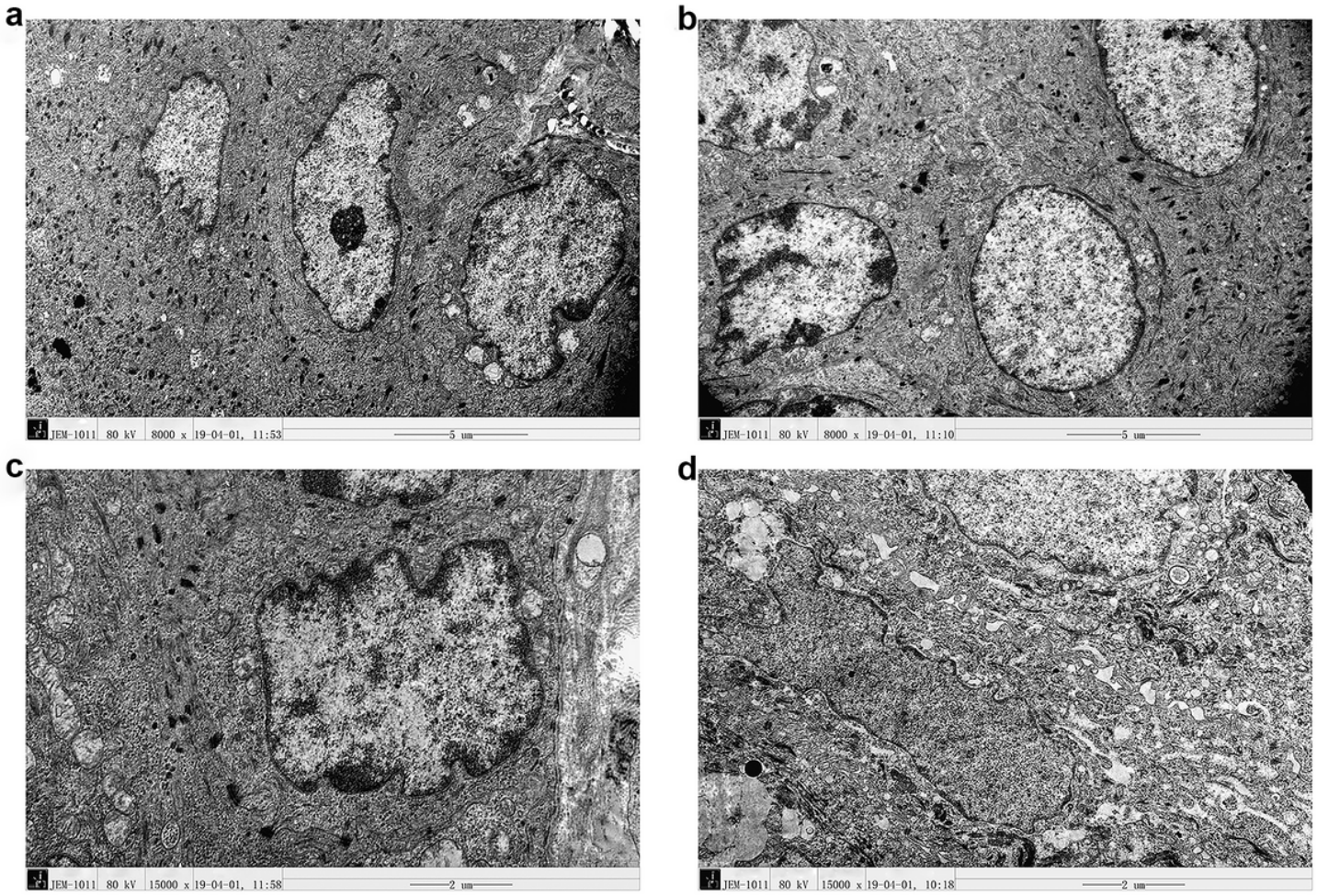


## Figure 2

Ultrastructural observation by Scanning Transmission Electron Microscopy (STEM). (a) Ultrastructural of blank control tissues. (b) Ultrastructural of simple hyperplasia tissues. (c) Ultrastructural of abnormal hyperplasia tissues. (d) Ultrastructural of carcinoma tissues.

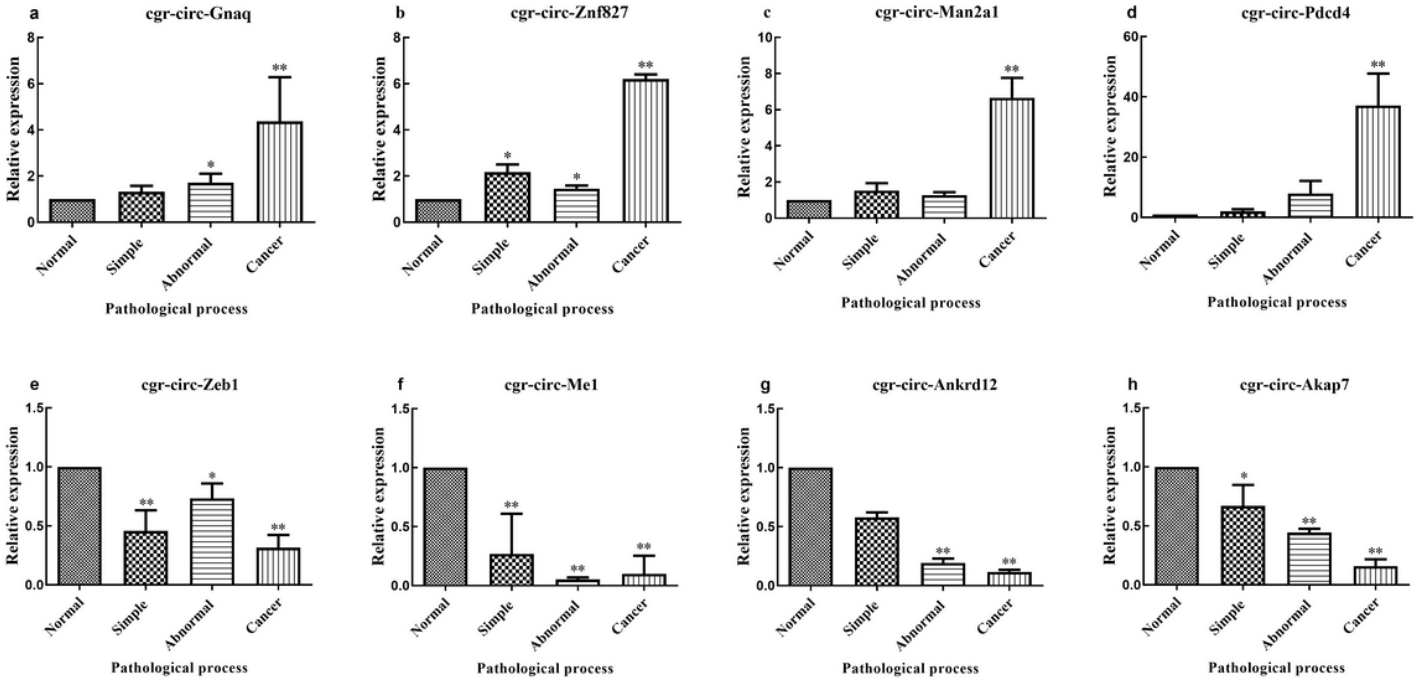


## Figure 3

qRT-PCR verification of the expression of circRNAs. The relative of the 8 circRNAs by real-time qPCR analysis in the 18 cheek pouch tissues from simple hyperplasia tissues, abnormal hyperplasia tissues and carcinoma tissues compared with normal tissues (a-h). (a) The expression of cgr-circ-Gnaq in four different pathological stages. (b) The expression of cgr-circ-Znf827 in four different pathological stages. (c) The expression of cgr-circ-Man2a1 in four different pathological stages. (d) The expression of cgr-circ-Pdcd4 in four different pathological stages. (e) The expression of cgr-circ-Zeb1 in four different pathological stages. (f) The expression of cgr-circ-Me1 in four different pathological stages. (g) The expression of cgr-circ-Ankrd12 in four different pathological stages. (h) The expression of cgr-circ-Akap7 in four different pathological stages. The levels of circRNAs from real-time qPCR were expressed as a ratio of 2-ΔΔCT. Data are expressed as means ± SD ($P<0.05$). Normal, normal tissues; simple, simple hyperplasia tissues; abnormal, abnormal hyperplasia tissues; cancer, carcinoma tissues.*$P<0.05$, **$P<0.01$.

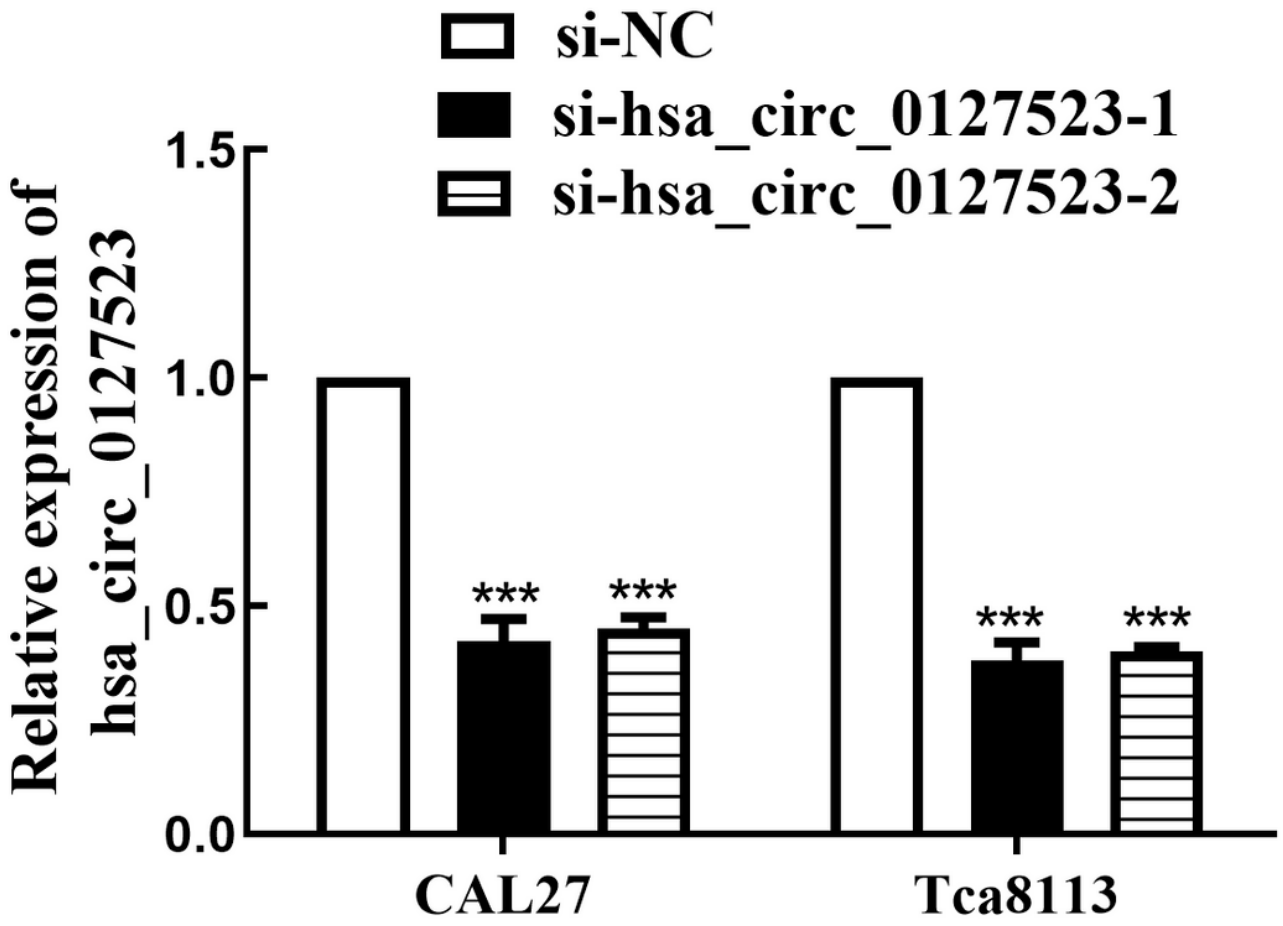


## Figure 4

Elevated transfection efficiency of si-hsa_circ_0127523-1 and si-hsa_circ_0127523-2 by qRT-PCR in OSCC cells. The expression level of si-hsa_circ_0127523-1 and si-hsa_circ_0127523-2 were significantly lower than that in the negative control group (Transient transfection si-NC in OSCC cells). ***P<0.001 vs. si-NC.

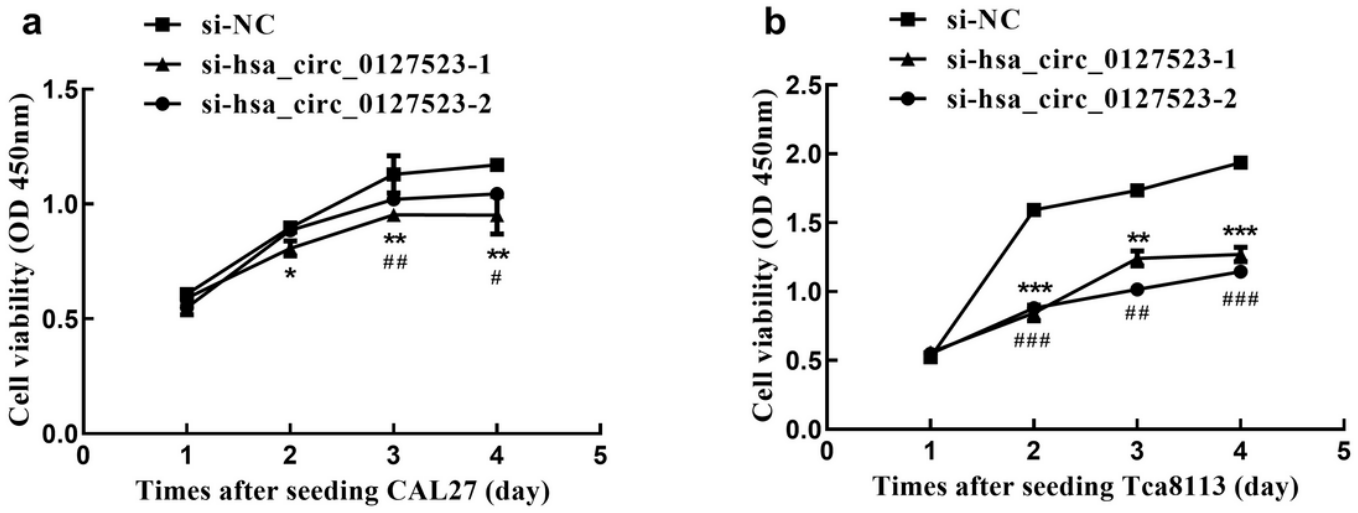

## Figure 5

Si-hsa_circ_0127523 inhibits proliferation ability of OSCC cells in vitro. (a) CAL 27 and (b) Tca8113 cells were transfection with negative control, si-hsa_circ_0127523-1 and si-hsa_circ_0127523-2, the CCK-8 assay was used to measure cell proliferation at different time points after cells seeding. Five replicate wells were used for each analysis. Error bars represent the mean ± SEM of three independent experiments. ***P<0.001, **P<0.01, *P<0.05 show si-hsa_circ_0127523-1 vs. si-NC; ###P<0.001, ##P<0.01, #P<0.05 show si-hsa_circ_0127523-2 vs. si-NC.

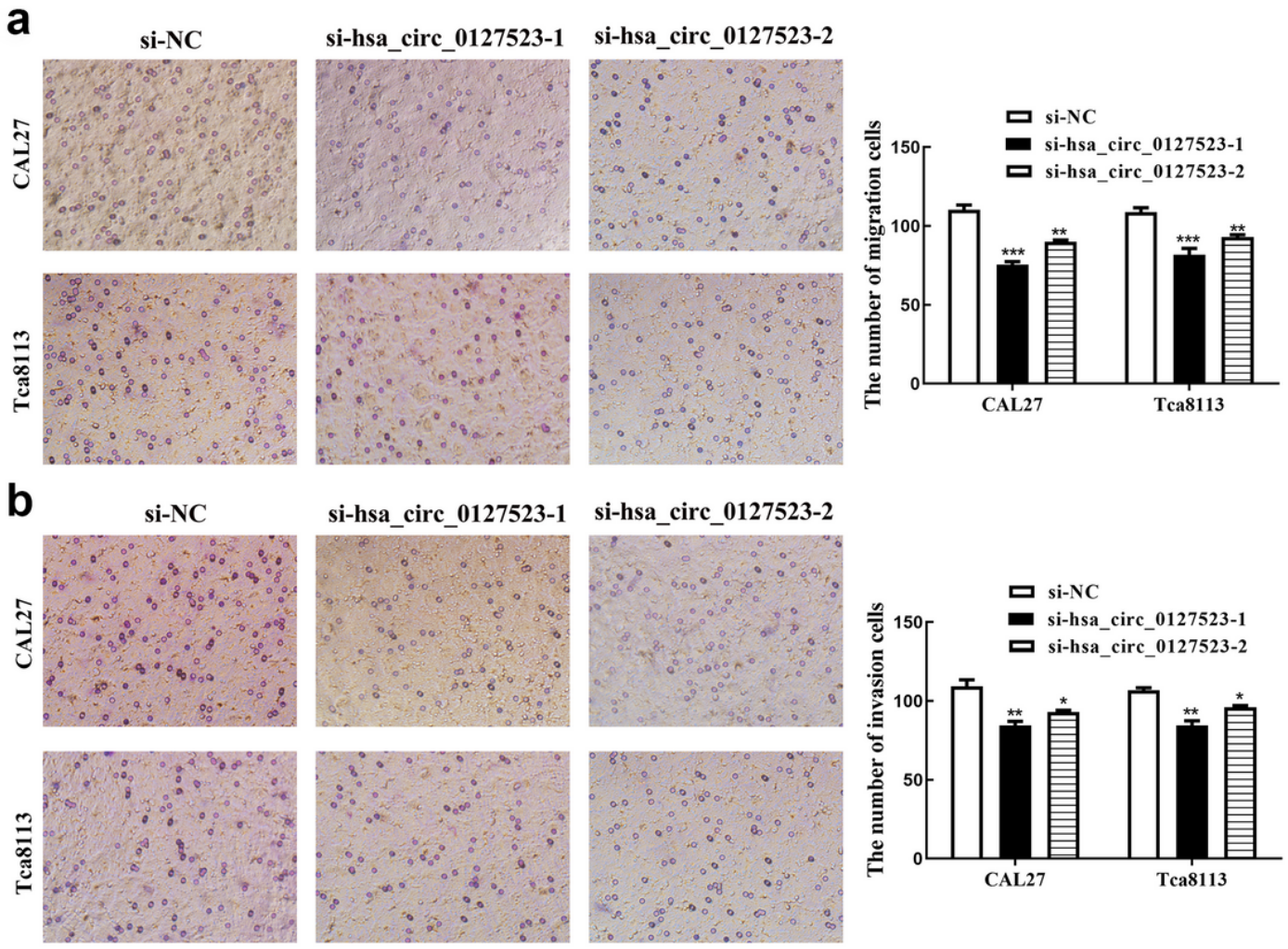


## Figure 6

Silencing of hsa_circ_0127523 represses the migration and invasion of CAL 27 and Tca8113 cells. (a) The cell migration capacity and migrative cell number was detected by transwell assays after transfection of negative control, si-hsa_circ_0127523-1 and si-hsa_circ_0127523-2 in CAL27 and Tca8113 cells. (b) The cell invasion capacity and invasive cell number was detected by transwell assays after transfection of negative control, si-hsa_circ_0127523-1 and si-hsa_circ_0127523-2 in CAL27 and Tca8113 cells. ***P<0.001, **P<0.01, *P<0.05 vs. si-NC.

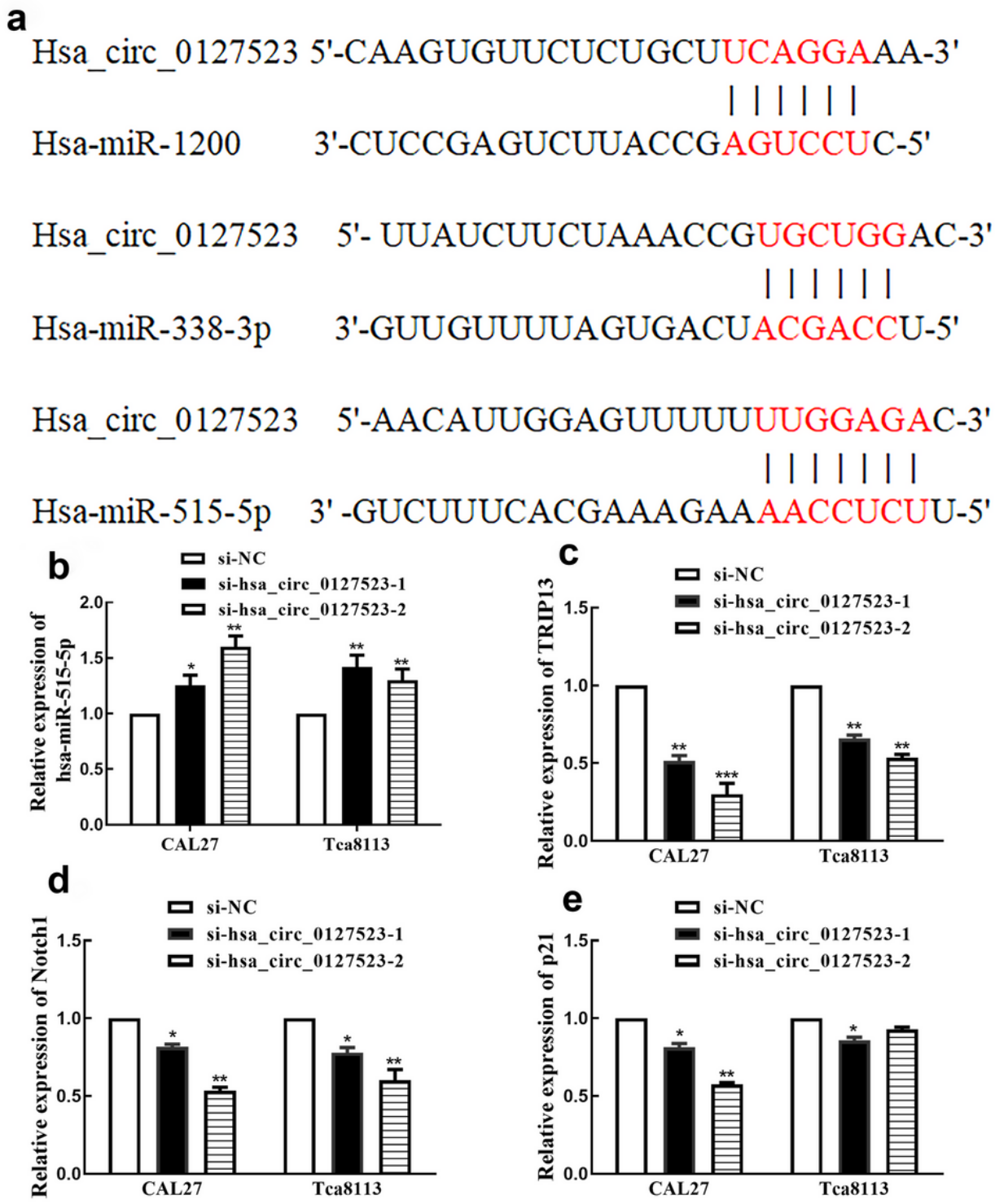


## Figure 7

Hsa-miR-515-5p was regulated by hsa_circ_0127523. (a) The predicted binding sites of hsa_circ_0127523 with hsa-miR-1200, hsa-miR-338-3p and hsa-miR-515-5p. CAL27 and Tca8113 cell lines were transfected with negative control and double siRNAs of hsa_circ_0127523, the relative expression level of hsa-miR-515-5p (b), TRIP13 (c), Notch1 (d) and p21 (e) were analyzed by qRT-PCR. ***P<0.001, **P<0.01, *P<0.05 vs. si-NC.

# Supplementary Files

This is a list of supplementary files associated with this preprint. Click to download.

- SupplementaryMaterial.pdf